

Supplemental Information

Structural transformations of the $\text{La}_{2-x}\text{Pr}_x\text{NiO}_{4+\delta}$ system probed by high-resolution synchrotron and neutron powder diffraction

Vaibhav Vibhu ^{a,b}, Matthew R. Suchomel ^{†a,b}, Nicolas Penin ^{a,b}, François Weill ^{a,b}, Jean-Claude Grenier ^{a,b}, Jean-Marc Bassat ^{a,b}, and Aline Rougier ^{a,b}

^a CNRS, ICMCB, UMR 5026, F-33600 Pessac, France

^b Univ. Bordeaux, ICMCB, UMR 5026, F-33600 Pessac, France

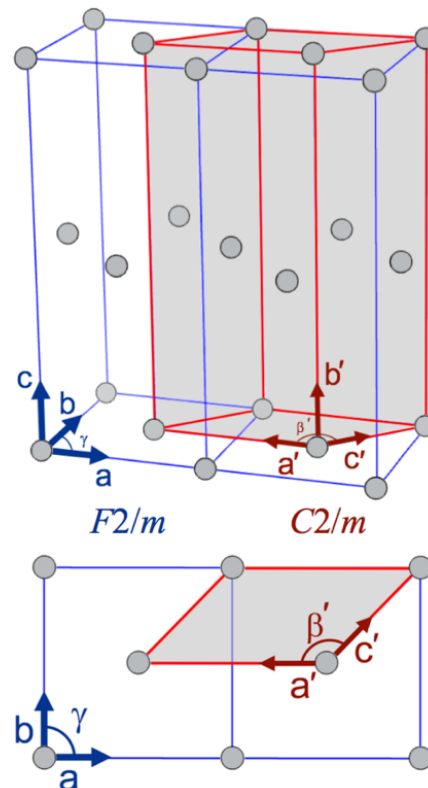
† Corresponding author

Transformation from
expanded $F2/m$ monoclinic cell to
standard $C2/m$ monoclinic cell
(Space Group #12, Setting: C 1 2/m 1)

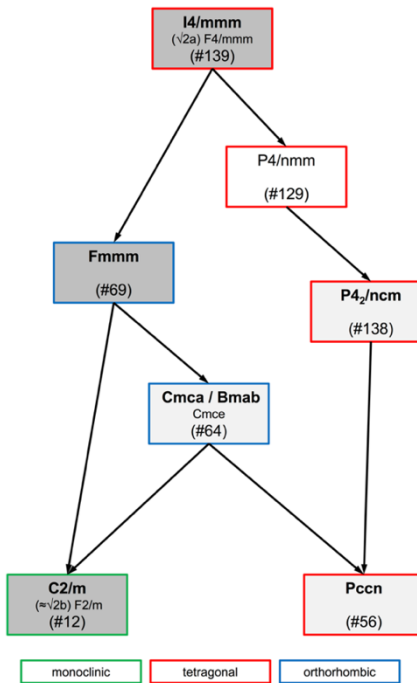
$$\begin{array}{ccc} F2/m & \rightarrow & C2/m \\ \left[\begin{array}{c} \textcolor{blue}{a} \\ \textcolor{blue}{b} \\ \textcolor{blue}{c} \end{array} \right] & = & \left[\begin{array}{c} \textcolor{red}{a}' \\ \textcolor{red}{b}' \\ \textcolor{red}{c}' \end{array} \right] \end{array}$$
$$\left[\begin{array}{ccc} -1 & 0 & 0 \\ 0 & 0 & 1 \\ 1/2 & 1/2 & 0 \end{array} \right]$$

Transformation for $\text{Pr}_2\text{NiO}_{4.25}$

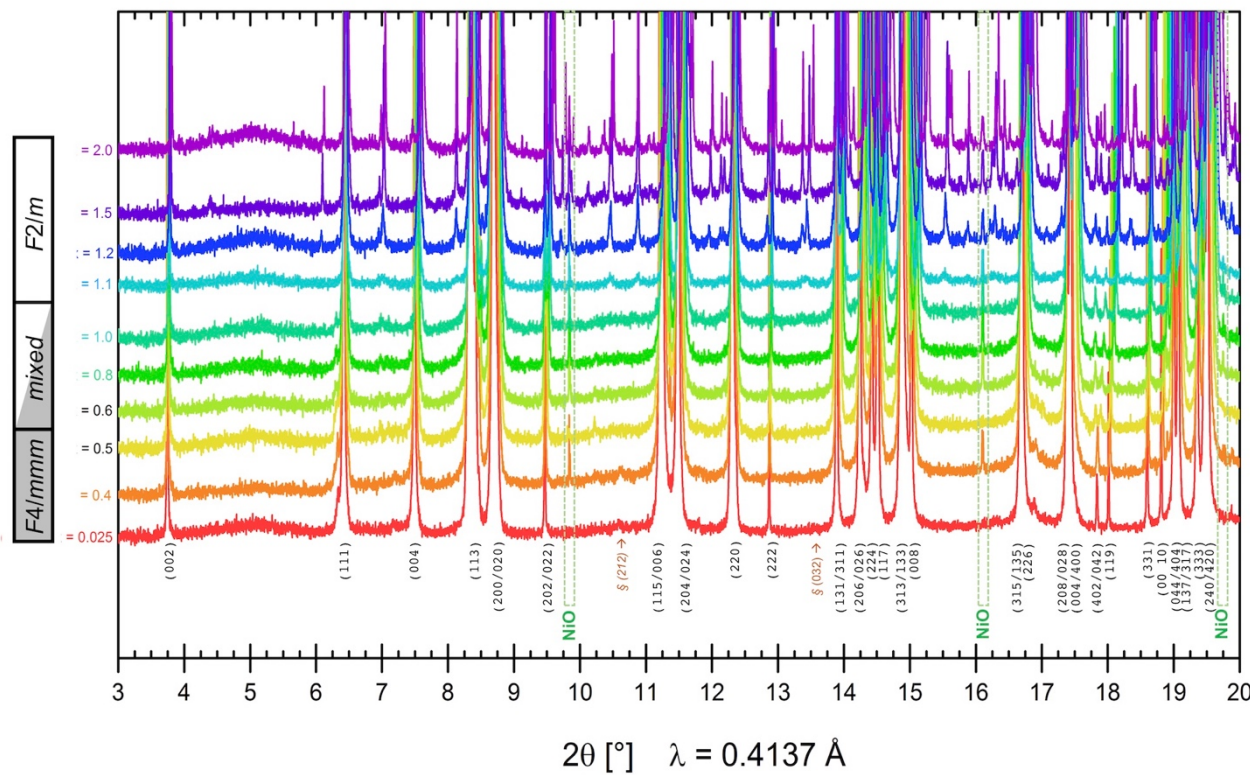
$F2/m$	\rightarrow	$C2/m$
$a = 5.3917 \text{ \AA}$		$a' = 5.3917 \text{ \AA}$
$b = 5.4574 \text{ \AA}$		$b' = 12.4478 \text{ \AA}$
$c = 12.4478 \text{ \AA}$		$c' = 3.8335 \text{ \AA}$
$\gamma = 90.07^\circ$		$\beta' = 134.62^\circ$
$V = 366.27 \text{ \AA}^3$		$V' = V/2 = 183.13 \text{ \AA}^3$
Pr @ (0, 0, 0.36)		Pr @ (0, 0.36, 0)
Ni @ (0, 0, 0)		Ni @ (0, 0, 0)
O1 @ (0, 0, 0.17)		O1 @ (0, 0.17, 0)
O2 @ ($\frac{1}{4}$, $\frac{1}{4}$, 0)		O2 @ (0, 0, $\frac{1}{2}$)
O3 @ ($\frac{3}{4}$, $\frac{1}{4}$, 0)		O3 @ ($\frac{1}{2}$, 0, $\frac{1}{2}$)
O4 @ ($\frac{1}{4}$, $\frac{1}{4}$, $\frac{1}{4}$)		O4 @ (0, $\frac{1}{4}$, $\frac{1}{2}$)



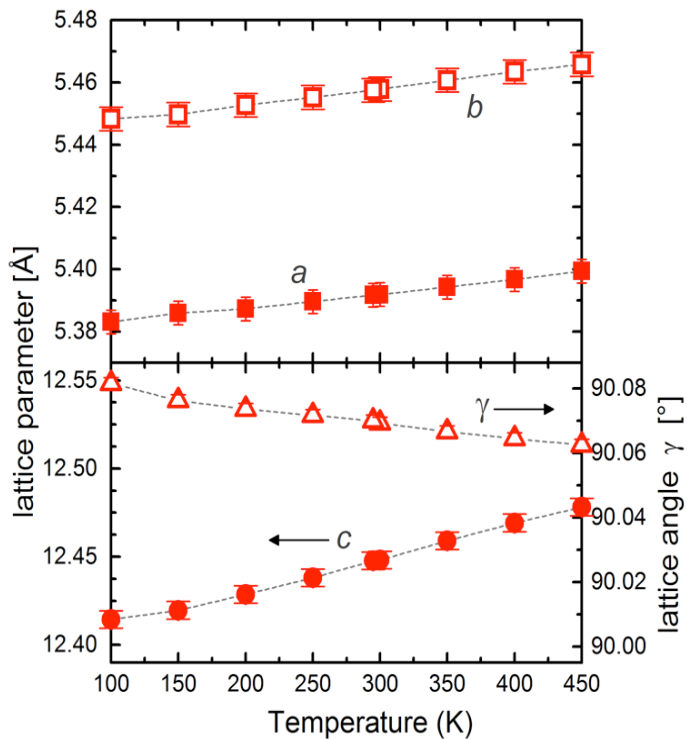
Supplemental Figure S1: Relationship between expanded $F2/m$ monoclinic unit cell (full name $F112/m$ with unique axis c) used in this work and its equivalent reduced conventional $C2/m$ cell in its standard crystallographic setting (full name $C12/m1$ with unique axis b). On the left, the transformation matrix is given, and corresponding lattice values and atomic positions are given for the $\text{Pr}_2\text{NiO}_{4.25}$ composition. On the right, a schematic diagram of the relationship between the $F2/m$ cell (in blue) and $C2/m$ cell (in red) is shown. For clarity, only the Ni atom is plotted in the unit cell.



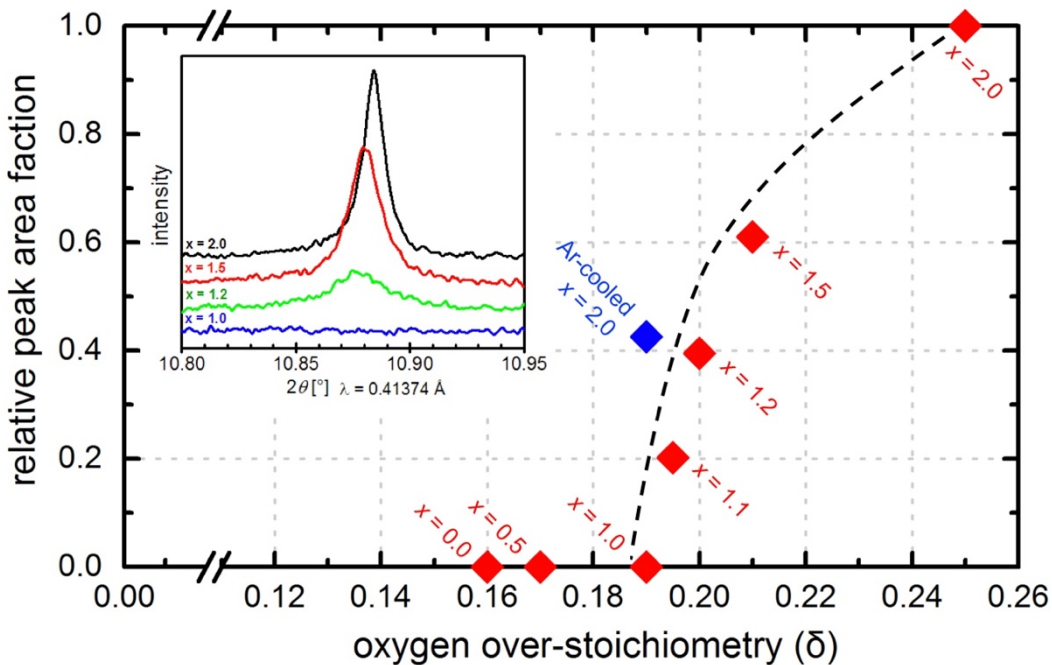
Supplemental Figure S2: Selected group/subgroup relationship paths between different space groups commonly referenced in the $\text{La}_2\text{NiO}_{4+\delta}$ and $\text{Pr}_2\text{NiO}_{4+\delta}$ literature; from the Bilbao Crystallographic Server⁵². Shaded space groups are reported for the LPNO system in the current study.



Supplemental Figure S3: Near background intensity zoomed view of HR-SPD data (295 K) for $\text{La}_{2-x}\text{Pr}_x\text{NiO}_{4+\delta}$ series. Assigned space groups in this study are marked on the left near the composition (x). Numerous weak intensity non-indexed peaks are clear for compositions with $x > 1.0$. Main peaks are labeled with hkl indexing for a generic F -centered orthorhombic cell (hkl condition; all even or all odd). Characteristic positions of (212) and (032) superlattice reflections allowed in $Bmab$ and $P4_2/ncm$ space groups that arise from ordered in-plane tilting of NiO_6 octahedra are marked by §. NiO impurity peaks (cubic $Fm\bar{3}m$ cell with $a = 4.176 \text{ \AA}$) are marked.



Supplemental Figure S4: Evolution of refined lattice parameters (a , b , c , γ) as a function of temperature for $\text{Pr}_2\text{NiO}_{4.25}$. Lattice values were obtained from refinements of *in-situ* variable temperature HR-SPD data using the $F2/m$ monoclinic unit cell.



Supplemental Figure S5: Evolution of the relative integrated peak area fraction observed in HR-SPD data at room temperature as a function of oxygen over-stoichiometry (δ) for Pr-rich $\text{La}_{2-x}\text{Pr}_x\text{NiO}_{4+\delta}$ compositions. The small inset upper figure plots the evolution of the reference non-indexed weak intensity peak (at $2\theta \approx 10.88^\circ$) for select air-cooled compositions. The integrated peak area was defined as 1.0 for $\delta = 0.25$, and normalized for each scan as a fraction of the integrated area for a $F2/m$ indexed (004) peak at $2\theta \approx 7.60^\circ$. Red plotted diamonds show air-cooled samples; the blue diamond represents the Ar-cooled $x = 2.0$ sample with reduced δ . The dashed black curve is a guide for the eye. See main text Section 4.4 for details and discussion.

Supplemental Table S1: Summary of Rietveld refined structural parameters and fit statistics for compositions (x) in the $\text{La}_{2-x}\text{Pr}_x\text{NiO}_{4+\delta}$ system. Refined values are followed by the uncertainty in brackets. The lack of an uncertainty value indicates a fixed non-refined parameter. Other symbols described in footnotes below.

Composition (x)	region of 2-phase coexistence												2.0 (Ar cooled) $F2/m$				
	0.0	0.25	0.4	0.5	0.6	0.8	1.0	1.1	1.2	1.5	2.0						
Space Group [†]	$Fmmm$	$F4/mmm$	$F4/mmm$	$F2/m$	$F4/mmm$	$F2/m$	$F4/mmm$	$F2/m$	$F4/mmm$	$F2/m$	$F2/m$						
weight fraction [▲]	--	--	--	0.66	0.34	0.76	0.24	0.84	0.16	0.92	0.08	--	--				
a (Å)	5.45985(1)	5.45992(1)	5.45700(1)	5.44209(2)	5.45492(2)	5.43737(2)	5.45279(3)	5.42874(1)	5.44904(2)	5.42111(1)	5.44482(2)	5.41771(1)	5.41440(1)	5.40572(1)	5.39172(1)	5.39757(1)	
b (Å)	5.46471(1)	= a	= a	5.46796(2)	= a	5.46892(2)	= a	5.46962(1)	= a	5.46904(1)	= a	5.46865(1)	5.46809(1)	5.46422(1)	5.45749(1)	5.45416(1)	
c (Å)	12.6862(2)	12.6582(1)	12.6414(1)	12.6396(3)	12.6315(2)	12.6195(2)	12.6207(1)	12.5939(1)	12.5952(1)	12.5706(2)	12.5702(1)	12.5572(2)	12.5443(1)	12.5091(1)	12.4478(1)	12.4386(2)	
g (°)	90	90	90	90.003(1)	90	90.003(2)	90	90.005(2)	90	90.010(2)	90	90.011(2)	90.026(2)	90.047(2)	90.070(2)	90.062(2)	
Vol. (Å ³), $Z = 4$	378.510(1)	377.351(1)	376.447(1)	375.888(1)	375.867(2)	375.259(1)	375.251(4)	373.994(1)	373.976(3)	372.695(1)	372.656(1)	372.036(1)	371.391(1)	369.495(1)	366.278(1)	366.181(1)	
Pr/La (0, 0, z)	0.36064	0.36046(1)	0.36040(1)	0.36042(4)	0.36020(5)	0.36025(3)	0.36036(9)	0.36024(3)	0.35946(9)	0.36017(2)	0.3584(2)	0.35993(2)	0.35994(2)	0.35960(2)	0.35910(2)	0.35958(2)	
fixed occupancy	La _{1.0}	Pr _{0.125} La _{0.87}	Pr _{0.20} La _{0.80}	Pr _{0.25} La _{0.75}	Pr _{0.30} La _{0.70}	Pr _{0.40} La _{0.60}	Pr _{0.50} La _{0.50}	Pr _{0.55} La _{0.45}	Pr _{0.60} La _{0.40}	Pr _{0.75} La _{0.25}	Pr _{1.0}	Pr _{1.0}					
$U_{iso} \times 100$ (Å ²)	0.75(1)	0.88(1)	0.91(1)		0.88(1)	0.82(1)	0.84(1)	0.85(1)		0.82*	0.91*	0.96*	0.95*		1.02(1)		
Ni (0, 0, 0)																	
$U_{iso} \times 100$ (Å ²)	0.32(1)	0.46(1)	0.48(1)		0.47(2)	0.52(2)	0.41(2)	0.41(1)		0.52*	0.59*	0.54*	0.55*		0.46(1)		
O(1) (0, 0, z)	0.1722(2)	0.1729(1)	0.1727(2)		0.1732(2)	0.1734(1)	0.1741(2)	0.1741(2)		0.1740(3)	0.1733(1)	0.1730(1)	0.1731(1)		0.1743(2)		
$U_{iso} \times 100$ (Å ²)	2.94(2)	2.9*	3.18*		4.1(2)	2.2(2)	4.78*	2.29*	3.8(1)	1.5(1)	4.65*	2.2(3)	5.00*	5.02*	5.29*	6.16*	3.96(6)
O(2) (1/4, 1/4, 0)																	
$U_{iso} \times 100$ (Å ²)	1.06(2)	0.86(4)	0.96(4)		1.17(5)	1.15(2)	0.93(5)	0.95(5)		0.96(6)	1.51*	1.45*	1.73*		1.51(6)		
O(3) (1/4, 1/4, 0)																	
$U_{iso} \times 100$ (Å ²)	--	--	--		1.17(5)	--	1.15(2)	0.93(5)		0.96(6)	1.66*	1.75*	1.76*		1.43(8)		
O(4) (1/4, 1/4, 1/4)																	
$U_{iso} \times 100$ (Å ²)	1.06(2)	0.86(4)	0.96(4)		1.17(5)	1.15(2)	0.93(5)	0.95(5)		1.5(3)	2.9(3)	2.9(3)	2.59(3)		2.6(1)		
occupancy	0.08	0.08	0.08		0.06(3)	0.08(2)	0.09(2)	0.09(2)		0.10(1)	0.11(1)	0.11(1)	0.12(1)		0.08(1)		
oxygen δ estimate [§]	0.16	0.16	0.16		0.17	0.17	0.18	0.19		0.20	0.20	0.21	0.25		0.19		
δ (diffraction)	0.16	0.16	0.16		0.13(5)	0.16(3)	0.18(3)	0.18(3)		0.20(2)	0.20(2)	0.22(2)	0.24(2)		0.17(2)		
δ (TGA)	0.16	--	--		0.17	--	--	0.19		--	--	0.21	0.25		0.19		
refined data sets [♦]	SPD	SPD	SPD		SPD	SPD+NPD	SPD	SPD		SPD	SPD+NPD	SPD+NPD	SPD+NPD		SPD		
SPD R_{wp}	9.68%	11.44%	10.73%		12.91%	13.62%	13.21%	13.87%		15.61%	13.46%	12.1%	12.8%		10.6%		
SPD+NPD R_{wp}	--	--	--		--	11.85%	--	--		10.97%	10.6%	10.4%		--			
Total Reduced χ^2	4.32	6.40	7.18		11.69	16.88	11.97	13.72		8.95	13.97	12.79	10.01		6.49		

Footnotes

[†] $F2/m$ (full name $F112/m$) is a non-standard setting of $C2/m$ (no 12); $F4/mmm$ is a non-standard $I4/mmm$ setting (no 139)

[▲] refined phase weight fractions for 2-phase compositions

[§] estimated oxygen δ values reported in Table 1; determined (primarily) from TGA data or from (secondarily) diffraction data structural refinements

* U_{iso} equivalent for refined U_{aniso} values (see supplemental information)

♦ Synchrotron Powder Diffraction (SPD), Neutron Powder Diffraction (NPD)

Supplemental Table S2: Summary of Rietveld refined anisotropic displacement parameter (ADP) values (U_{aniso}) for selected Pr-rich compositions (x) in the $\text{La}_{2-x}\text{Pr}_x\text{NiO}_{4+\delta}$ system.

Composition (x)	1.1	1.2	1.5	2.0
Space Group	$F2/m$	$F2/m$	$F2/m$	$F2/m$
refined data sets	SPD	SPD+NPD	SPD+NPD	SPD+NPD
Pr/La: $U_{aniso} \times 100 (\text{\AA}^2)$				
U11	0.69(1)	0.77(1)	0.85(1)	0.84(1)
U22	0.99(1)	1.19(1)	1.26(1)	1.34(1)
U33	0.74(1)	0.76(1)	0.75(1)	0.67(1)
U12	-0.18(4)	-0.14(1)	-0.22(1)	-0.24(1)
Ni: $U_{aniso} \times 100 (\text{\AA}^2)$				
U11	0.23(4)	0.37(2)	0.26(2)	0.22(2)
U22	0.16(4)	0.32(3)	0.30(2)	0.25(2)
U33	0.92(4)	1.07(2)	1.05(2)	1.17(3)
U12	-0.2(1)	-0.25(3)	0.18(3)	-1.10(3)
O(1): $U_{aniso} \times 100 (\text{\AA}^2)$				
U11	4.9(3)	5.30(8)	5.23(8)	5.91(8)
U22	9.9(4)	9.15(12)	10.06(12)	11.90(12)
U33	0.1(2)	0.61(5)	0.59(5)	0.69(5)
U12	6.4(4)	6.02(11)	5.30(12)	5.41(13)
O(2): $U_{aniso} \times 100 (\text{\AA}^2)$				
U11	--	0.90(11)	0.71(14)	0.82(11)
U22	--	0.31(13)	0.27(14)	0.33(11)
U33	--	3.63(30)	3.36(31)	4.14(29)
U12	--	-0.40(8)	-0.27(8)	-0.25(7)
O(3): $U_{aniso} \times 100 (\text{\AA}^2)$				
U11	--	0.39(10)	0.34(13)	0.26(10)
U22	--	0.95(12)	0.57(15)	0.53(11)
U33	--	3.64(33)	4.34(35)	4.38(30)
U12	--	0.18(7)	0.21(8)	0.21(6)

Supplemental Table S3: Summary of selected bond distances determined from Rietveld refined structural models for compositions (x) in the $\text{La}_{2-x}\text{Pr}_x\text{NiO}_{4+\delta}$ system.

Composition (x)	region of 2-phase coexistence												2.0 (Ar cooled)																		
	0.0			0.25			0.4			0.5			0.6			0.8			1.0			1.1			1.2			1.5			
	Space Group	$Fmmm$	$F4/mmm$	$F4/mmm$	$F2/m$	$F4/mmm$	$F2/m$	$F4/mmm$	$F2/m$	$F4/mmm$	$F2/m$	$F4/mmm$	$F2/m$	$F4/mmm$	$F2/m$	$F4/mmm$	$F2/m$	$F4/mmm$	$F2/m$	$F4/mmm$	$F2/m$	$F4/mmm$	$F2/m$	$F4/mmm$	$F2/m$	$F4/mmm$	$F2/m$				
refined data sets	SPD	SPD	SPD	SPD	SPD	SPD+NPD	SPD	SPD	SPD	SPD	SPD	SPD	SPD	SPD	SPD	SPD	SPD	SPD	SPD	SPD	SPD	SPD	SPD	SPD	SPD	SPD	SPD				
Ni-O(1) ($x2$)	2.198(2)	2.188(2)	2.183(2)	2.188(3)	2.188(3)	2.188(2)	2.1878(2)	2.193(3)	2.193(3)	2.1886(2)	2.189(2)	2.185(3)	2.173(1)	2.164(1)	2.155(1)	2.168(3)	2.168(3)	2.168(3)	2.168(3)	2.168(3)	2.168(3)	2.168(3)	2.168(3)	2.168(3)	2.168(3)	2.168(3)	2.168(3)				
Ni-O(2) ($x2$, $x4$) †	1.9312(2)	1.9304(2)	1.9293(2)	1.9286(1)	1.9286(1)	1.9278(1)	1.9282(1)	1.9265(1)	1.9265(1)	1.9249(1)	1.9250(2)	1.9243(3)	1.9233(1)	1.9208(1)	1.9167(1)	1.9173(1)	1.9173(1)	1.9173(1)	1.9173(1)	1.9173(1)	1.9173(1)	1.9173(1)	1.9173(1)	1.9173(1)	1.9173(1)	1.9173(1)	1.9173(1)				
Ni-O(3) ($x2$)	--	--	--	--	--	1.9287(1)	--	1.9278(1)	--	1.9268(1)	--	1.9253(2)	1.9246(3)	1.9242(1)	1.9224(1)	1.9191(1)	1.9194(1)	1.9194(1)	1.9194(1)	1.9194(1)	1.9194(1)	1.9194(1)	1.9194(1)	1.9194(1)	1.9194(1)	1.9194(1)	1.9194(1)				
Pr/La-O(1) ($x1$)	2.378(2)	2.374(2)	2.373(2)	2.362(3)	2.365(3)	2.359(2)	2.359(2)	2.334(3)	2.344(3)	2.316(2)	2.3388(3)	2.335(3)	2.3417(2)	2.3338(2)	2.315(2)	2.305(3)	2.305(3)	2.305(3)	2.305(3)	2.305(3)	2.305(3)	2.305(3)	2.305(3)	2.305(3)	2.305(3)	2.305(3)	2.305(3)				
Pr/La-O(1) ($x2$, $x4$) †	2.7635(3)	2.7624(3)	2.7604(3)	2.7599(4)	2.7668(4)	2.7592(3)	2.7672(2)	2.7572(4)	2.7689(4)	2.7527(3)	2.7683(2)	2.7673(5)	2.7656(2)	2.7624(2)	2.7581(2)	2.7594(4)	2.7594(4)	2.7594(4)	2.7594(4)	2.7594(4)	2.7594(4)	2.7594(4)	2.7594(4)	2.7594(4)	2.7594(4)	2.7594(4)	2.7594(4)				
Pr/La-O(1) ($x2$)	--	--	--	--	--	2.7540(4)	--	2.7516(2)	--	2.7487(4)	--	2.7445(1)	2.7422(5)	2.7390(2)	2.7335(2)	2.7255(2)	2.7315(4)	2.7315(4)	2.7315(4)	2.7315(4)	2.7315(4)	2.7315(4)	2.7315(4)	2.7315(4)	2.7315(4)	2.7315(4)	2.7315(4)				
Pr/La-O(2) ($x2$, $x4$) †	2.6182(2)	2.6166(2)	2.6147(1)	2.6149(4)	2.6131(3)	2.6129(8)	2.6126(3)	2.6163(8)	2.6097(2)	2.6220(14)	2.6070(2)	2.6070(2)	2.6050(2)	2.6039(2)	2.5998(2)	2.5936(1)	2.5936(1)	2.5936(1)	2.5936(1)	2.5936(1)	2.5936(1)	2.5936(1)	2.5936(1)	2.5936(1)	2.5936(1)	2.5936(1)	2.5936(1)				
Pr/La-O(3) ($x2$)	--	--	--	--	--	2.6132(3)	--	2.6128(3)	--	2.6096(2)	--	2.6068(2)	2.6073(2)	2.6027(2)	2.5981(2)	2.5951(1)	2.5951(1)	2.5951(1)	2.5951(1)	2.5951(1)	2.5951(1)	2.5951(1)	2.5951(1)	2.5951(1)	2.5951(1)	2.5951(1)					
Pr/La-O(4) ($x2$)	2.3874(2)	2.3835(1)	2.3812(2)	2.3785(4)	2.3801(3)	2.3776(7)	2.3776(2)	2.3690(7)	2.3748(2)	2.3582(12)	2.3714(2)	2.3682(2)	2.3667(2)	2.3599(2)	2.3491(2)	2.3525(1)	2.3525(1)	2.3525(1)	2.3525(1)	2.3525(1)	2.3525(1)	2.3525(1)	2.3525(1)	2.3525(1)	2.3525(1)	2.3525(1)					
Pr/La-O(4) ($x2$)	2.3874(2)	2.3835(1)	2.3812(2)	2.3785(4)	2.3802(3)	2.3776(7)	2.3779(2)	2.3690(7)	2.3749(2)	2.3582(12)	2.3716(2)	2.3685(2)	2.3674(2)	2.3612(2)	2.3510(2)	2.3542(1)	2.3542(1)	2.3542(1)	2.3542(1)	2.3542(1)	2.3542(1)	2.3542(1)	2.3542(1)	2.3542(1)	2.3542(1)	2.3542(1)					

† Bond multiplicity is $x2$ for $F2/m$, but $x4$ for $F4/mmm$ and $Fmmm$ models, where O(2) and O(3) sites are equivalent